Designing Lubricant-Impregnated Surfaces for Corrosion Protection

Sami Khan[‡,*] *and Kripa K. Varanasi*[**]

Corrosion is a detrimental process that can impact the performance and lifetime of many infrastructural systems. In this research, lubricant-impregnated surfaces (LIS) for corrosion protection are systematically developed and studied. Using microtextures with controlled geometry and spacing, this study shows that the corrosion resistance on LIS is greatly enhanced compared to bare iron as determined by a reduction in the corrosion current density by three orders of magnitude. Furthermore, it shows that the spreading characteristics of the lubricant are important toward ensuring effective corrosion protection. Krytox, a lubricant that covers both inside the textures as well as the top of the textures, provides two orders of magnitude greater corrosion protection as compared to silicone oil that does not cover texture tops. The practical applicability of LIS are highlighted to demonstrate corrosion protection on carbon steel in brine.

KEY WORDS: carbon steel, coatings, interfacial effects, surface tension

INTRODUCTION

It is estimated that the total direct costs related to corrosion are $121 billion, or about 1.38% of the U.S. gross domestic product (GDP).[1] Protective coatings alone account for 88% of these costs, which include the raw materials to make the coatings as well as the costs associated with replacing damaged coatings on a yearly basis.[1] A vast majority of corrosion research has been devoted to developing coatings that can reduce corrosion.[1-2] These protective coatings act as barriers that reduce the contact between the corrosive media and the underlying metal surface, however, any mechanical defects such as cracks or holes formed over time within the coating can provide pathways for corrosion.

A lubricant-impregnated surface (LIS) is a hybrid coating whereby a textured scaffold is coated with a hydrophobic modifier and then impregnated with a liquid lubricant which is stabilized by capillary and intermolecular forces.[3-9] The hydrophobic modifier lowers the surface energy of the substrate and ensures that the lubricant is not displaced by water atop (see Figure 1), thereby making these surfaces remarkably slippery. The thickness of the lubricant is dictated by the size of the textured features as well as the lubricant viscosity, surface tension, and coating speed,[10-11] and a controlled process to make LIS typically results in an equilibrium lubricant film that strongly adheres to the baseline substrate. Various methods for texturing LIS substrates both at the micro- and nanoscale have been developed.[12-13]

Owing to their unique properties and composite liquid-solid features, LIS technology has found applications in minimizing ice adhesion,[11] drag reduction,[14-15] and mitigating scale formation.[16-17] LIS systems offer promise in corrosion protection because unlike solid coatings, holes and cracks do not form in lubricant layers. Numerous papers have studied combinations of lubricants and porous and textured surfaces under various corrosive environments.[18-22] However, it is unclear if the lubricant films used in these studies were specifically controlled for equilibrium thickness, which is only obtained if the LIS is prepared using a controlled impregnation process that carefully considers the lubricant's properties and speed of application.[10-11] Lubricant films having thicknesses greater than equilibrium thin films may impart full surface coverage and provide temporary corrosion protection, but as thick films are not stabilized by capillary forces the lubricant can drain by gravity and other forces, consequently affecting corrosion protection.[23] In addition, many previous studies used a hydrophobic surface modifier such as Teflon[†] that itself can contribute directly to the barrier resistance on the surface, thereby making it harder to isolate the true effect of the lubricant on corrosion protection. This warrants a more thorough investigation of LIS with systematic texture geometries and lubricant properties for corrosion protection, which is presented in this study.

EXPERIMENTAL PROCEDURES

2.1 | Preparing Textured Coupons for Corrosion Testing

Lubricant-impregnated surfaces were developed on textured silicon substrates. Silicon was chosen as the base material as it is relatively easier to pattern micropillars on silicon as compared to other materials such as steel. A silicon wafer (6 in [15.24 cm] diameter) was textured using photolithography, and the resulting micropillars had a cubical geometry with width a = 10 μm, height h = 10 μm, and pitch b = 10 μm (see Figure 1[b]).

Silicon is not typically susceptible to corrosion unless it is immersed in extremely strong bases or acids under

Submitted for publication: September 14, 2020. Revised and accepted: October 6, 2020. Preprint available online: October 6, 2020, https://doi.org/10.5006/3690.
‡ Corresponding author. E-mail: s_khan@sfu.ca; varanasi@mit.edu.
* Simon Fraser University, School of Sustainable Energy Engineering, Surrey, BC, Canada.
** Massachusetts Institute of Technology, Department of Mechanical Engineering, Cambridge, Massachusetts.
† Trade name.

ISSN 0010-9312 (print), 1938-159X (online) © 2020 NACE International. Reproduction or redistribution of this article in any form is prohibited without express permission from the publisher.

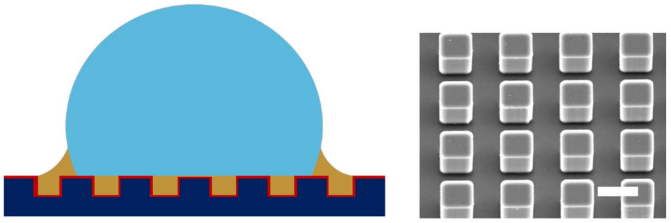

(a) (b)

FIGURE 1. *(a) Schematic of LIS showing a drop of water sitting atop a textured surface (dark blue) coated with a hydrophobic modifier (red layer) and impregnated with a lubricant (yellow). (b) Scanning electron microscopy (SEM) image of a microtextured surface on silicon showing pillars with width a = 10 µm, height h = 10 µm, and pitch b = 10 µm. Scale bar: 15 µm.*

high-temperature and pressure conditions, which are dangerous for a systematic corrosion study. Hence, in order to adapt the silicon surface to a more industrially-relevant material that can be tested for corrosion in 3.5 wt% sodium chloride, the silicon wafer was coated conformally with a 0.5 µm layer of iron using sputter-deposition. The wafer was then diced into 1 in by 1 in squares (2.54 cm by 2.54 cm) and the resulting test coupons mimicked the underlying texture on silicon. To confirm the susceptibility of the iron coating, both smooth and textured coupons were exposed to 0.1 M hydrochloric acid and observed under an optical microscope, as shown in Figure 2. The films rapidly deteriorated and bubbles evolved thereby confirming the suitability of these films for corrosion testing.

2.2 | Preparing Lubricant-Impregnated Surfaces

In order to design an LIS system for use in corrosion protection, (1) the lubricant should be immiscible with the corrosive test fluid, (2) the lubricant itself should be electrochemically inactive, and (3) the lubricant should preferentially wet the textured surface in the presence of the corrosive fluid. Two lubricants that have been previously shown in electrochemical studies to meet these criteria were selected in this research to prepare LIS: Krytox GPL 102† (hereafter commercial lubricant) and silicone oil.[24] To reduce the surface energy of the test coupons and to make them suitable for impregnating with these lubricants, a special hydrophobic modifier namely fluorophosphonic acid (FPA) was applied. FPA forms a thin monolayer by binding with iron atoms,[25] and hydrophobicity was confirmed by measuring the contact angle of water on a smooth FPA-coated iron substrate: 98±3°. Following FPA deposition, the coupons were impregnated with the lubricant using a controlled dip-coating process described elsewhere,[10-11] thereby resulting in equilibrium lubricant films.

2.3 | Potentiodynamic Polarization Experiments

All potentiodynamic corrosion experiments were conducted using a Biologic VSP† potentiostat in a three-electrode cell with 3.5 wt% sodium chloride as the test electrolyte and a standard Ag/AgCl reference electrode and an inert graphite counter electrode. The electrical connection was made on an area of the coupon that was not covered with FPA or lubricant. For all samples tested, a fixed geometric area of 0.5 cm^2 was immersed in the electrolyte. The micropillars provided additional surface roughness, which increased the geometric area of the substrate by a factor of 2.[4] Hence, an actual electrochemically active area of 1 cm^2 was used for the corrosion current density calculations. After immersing in the electrolyte, the open-circuit potential (OCP) was allowed to stabilize for at least 1 h before testing. Potentiodynamic scans were conducted around the OCP with a 1 mV/s scan rate, and the corrosion current was determined from the Tafel fitting of the resulting plot.

RESULTS AND DISCUSSION

3.1 | Spreading Lubricant-Impregnated Surface and Nonspreading Lubricant-Impregnated Surface

The contact angle of the impregnating lubricant (o) on the solid (s) in the presence of the corrosive electrolyte (w), $\theta_{os(w)}$, characterizes how the lubricant preferentially adheres to the solid in the presence of the corrosive electrolyte.[4] In the case of complete spreading of the lubricant on the surface, the lubricant is not only stably impregnated within the textures but also covers the tops of the texture as a thin equilibrium film, which results in $\theta_{os(w)} = 0°$. This LIS state is called a "spreading LIS" (see Figure 3[a]). In contrast, in a "nonspreading LIS", $\theta_{os(w)} > 0°$. This results in the post tops being exposed (see Figure 3[c]). Nevertheless, for nonspreading LIS, stable impregnation within the textures is still possible and the specific thermodynamic criteria that govern the formation of these states based on the spreading coefficient have been described in previous literature.[4,23]

The well-defined nature of micropillars developed in this study allowed explicit identification of both spreading and nonspreading LIS systems. The contact angles of both the

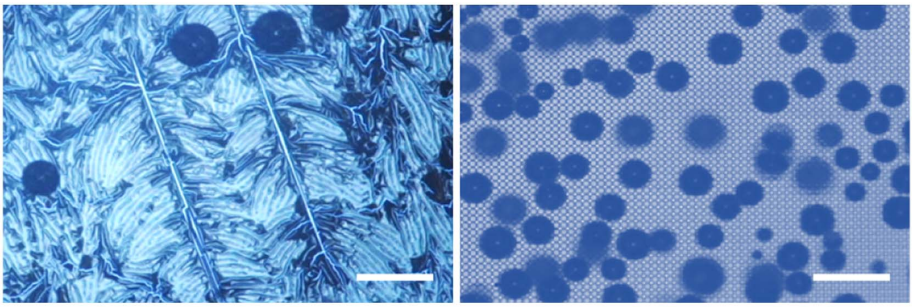

(a) (b)

FIGURE 2. *(a) A thin film of iron (0.5 µm) on a smooth silicon wafer deteriorating when exposed to 0.1 M HCl, evolving hydrogen gas bubbles. (b) Iron film of the same thickness conformally deposited on textured silicon as shown in Figure 1(b), demonstrating even more vigorous bubbling when exposed to 0.1 M HCl. Scale bars are 100 µm.*

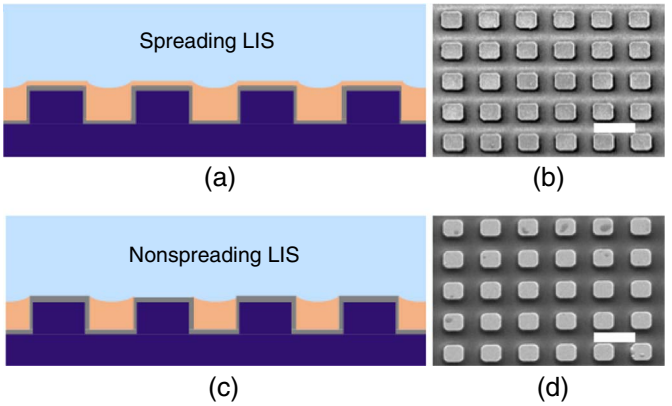

FIGURE 3. *(a) Schematic showing a spreading LIS which covers both the tops and within the textures. (b) SEM image showing consistent lubricant coverage using the commercial lubricant which forms a spreading LIS. (c) Schematic showing a nonspreading LIS where the texture tops are exposed. (d) SEM image showing the nonspreading LIS made using silicone oil, showing discrete lubricant drops on top of posts. Scale bars shown are 20 μm.*

commercial lubricant and silicone oil were measured on a smooth iron coupon coated with FPA in the presence of 3.5 wt% NaCl ($\theta_{os(w)}$). The commercial lubricant showed $\theta_{os(w)} = 0°$, while silicone oil showed $\theta_{os(w)} = 30\pm2°$. Therefore, with the commercial lubricant, a spreading LIS was obtained where the lubricant covered both the tops and inside the textures (see SEM image in Figure 3[b]), while silicone oil resulted in a nonspreading LIS. Discrete lubricant droplets were observed on top of the posts, as shown in Figure 3(d), indicating that the lubricant film was not stable on top of posts, thereby resulting in a nonspreading LIS.

3.2 | Potentiodynamic Polarization

Figure 4(a) shows the potentiodynamic polarization plots obtained using four test samples: (1) bare iron, (2) iron coated with the FPA hydrophobic modifier, (3) spreading LIS using the commercial lubricant, and (4) nonspreading LIS using silicone oil. Figure 4(b) compares the corrosion current densities as determined from the polarization plots. These currents were corrected for the ohmic resistance, which for both LIS cases represented less than 3% of the polarization resistance. It can be seen that both LIS systems—spreading and nonspreading—significantly reduce the corrosion current density relative to iron: from three orders of magnitude reduction with spreading LIS to one order of magnitude reduction with nonspreading LIS. It is also interesting to note that the corrosion current density of the iron coupon coated with the hydrophobic modifier FPA is found to be the same order of magnitude as that of iron. This confirms that any corrosion resistance characterization in this study for LIS is obtained only from the lubricant, and not from the hydrophobic modifier itself, in contrast with previous studies.

These results highlight the importance of determining the type of LIS toward ensuring effective corrosion protection. A spreading LIS with complete coverage of an equilibrium lubricant film provides superior corrosion protection as the lubricant always adheres to the surface both within and atop the textures. In contrast, even though a nonspreading LIS holds the lubricant stably within the textures, corrosion protection is reduced as the discrete drops atop the textures seen in Figure 3(d) are displaced by the corrosive electrolyte, thereby exposing the tops. A thicker lubricant film may temporarily provide corrosion protection but the lubricant layer on top of the posts is unstable and can drain over time. Therefore, it is important to systematically design LIS with full consideration of the lubricant's spreading properties to ensure optimal corrosion protection.

3.3 | Lubricant-Impregnated Surface on Carbon Steel

To demonstrate the practical applicability of LIS, corrosion was studied on carbon steel, a commonly used industrial alloy, in a 3.5 wt% NaCl solution (brine). Microscale roughness was achieved by sandblasting a 1 in by 1.5 in (2.54 cm by 3.81 cm) carbon steel coupon, and the surface energy was lowered using FPA followed by dipcoating with the commercial lubricant. As shown in Figure 3(e), the LIS sample did not corrode even after 48 h of exposure. This shows that when systematically designed, LIS can provide protection even on an industrially relevant surface. Ideally, LIS is best suited for protection of static components (such as the interior of storage vessels) with periodic replenishment of the lubricant during maintenance cycles.

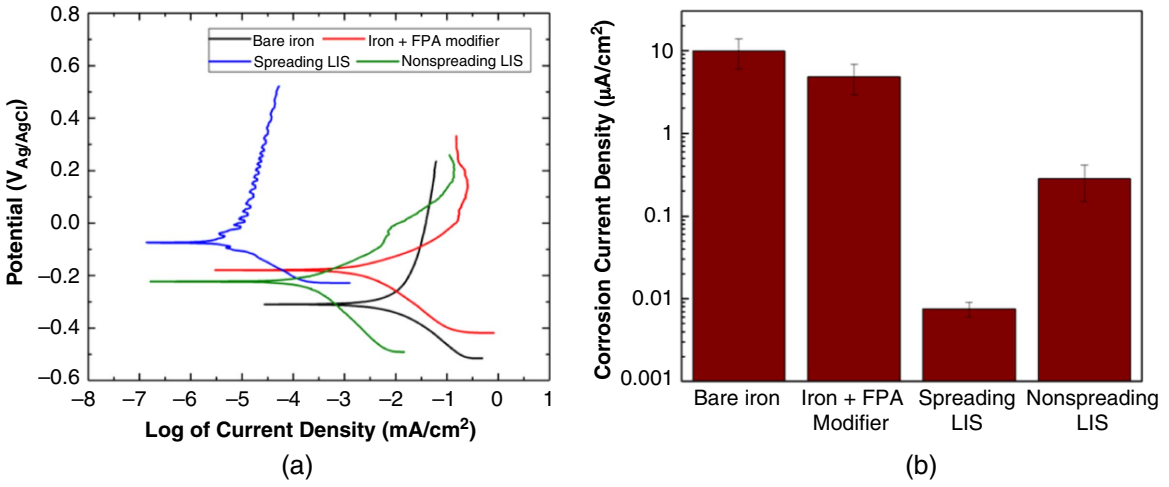

FIGURE 4. *(a) Potentiodynamic polarization curves showing the open-circuit potential and (b) corrosion current density as determined from the potentiodynamic curves.*

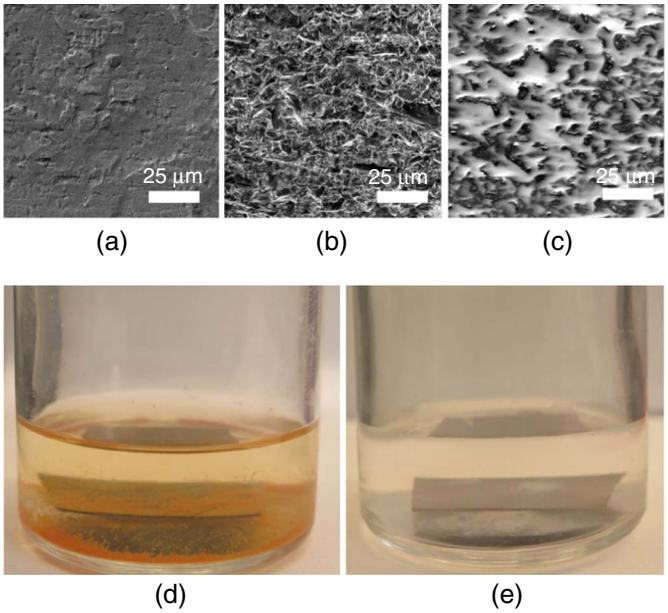

FIGURE 5. *SEM images showing: (a) as-received carbon steel coupon, (b) sand-blasted coupon with micrometric roughness features, (c) the commercial lubricant-based spreading LIS developed on the textured coupon, (d) control coupon corroding after 48 h of exposure to 3.5 wt% NaCl, and (e) LIS-coated coupon showing no corrosion after 48 h.*

SUMMARY

➢ In summary, corrosion protection on well-defined lubricant-impregnated surfaces has been systematically studied, finding that LIS offers superior corrosion protection when compared to bare iron in 3.5 wt% sodium chloride. It has been shown that this corrosion protection results exclusively from the protective lubricant layer rather than the hydrophobic barrier coating that is typically applied to ensure stability of LIS. Furthermore, it has been shown that the spreading characteristics of the lubricant is important toward optimal corrosion protection. When coated on carbon steel, LIS has been shown to provide lasting protection when exposed to brine.

ACKNOWLEDGMENTS

The authors gratefully acknowledge financial support from NSERC Canada (PGS-D Award) and the MITEI-Equinor grant. The authors thank Thomas Allison and Jacky Chin for their assistance in surface fabrication and characterization.

References

1. G.H. Koch, M. Bringers, N. Thompson, "Corrosion Costs and Preventive Strategies in the United States," NACE International, 2004.
2. E.P. Banczek, P.R.P. Rodrigues, I. Costa, *Surf. Coat. Technol.* 202, 10 (2008): p. 2008-2014.
3. D. Quéré, *Rep. Prog. Phys.* 68, 11 (2005): p. 2495-2532.
4. J.D. Smith, R. Dhiman, S. Anand, E. Reza-Garduno, R.E. Cohen, G.H. McKinley, K.K. Varanasi, *Soft Matter* 9, 6 (2013): p. 1772.
5. A. Lafuma, D. Quéré, *Europhys. Lett.* 96, 5 (2011): p. 56001.
6. T.-S. Wong, S.H. Kang, S.K.Y. Tang, E.J. Smythe, B.D. Hatton, A. Grinthal, J. Aizenberg, *Nature* 477, 7365 (2011): p. 443-447.
7. F. Schellenberger, J. Xie, N. Encinas, A. Hardy, M. Klapper, P. Papadopoulos, H.-J. Butt, D. Vollmer, *Soft Matter* 11, 38 (2015): p. 7617-7626.
8. A. Carlson, P. Kim, G. Amberg, H.A. Stone, *Europhys. Lett.* 104, 3 (2013): p. 34008.
9. A. Eifert, D. Paulssen, S.N. Varanakkottu, T. Baier, S. Hardt, *Adv. Mater. Interfaces* 1, 3 (2014): p. 1300138.
10. J. Seiwert, C. Clanet, D. Quéré, *J. Fluid Mech.* 669 (2011): p. 55-63.
11. S.B. Subramanyam, K. Rykaczewski, K.K. Varanasi, *Langmuir* 29, 44 (2013): p. 13414-13418.
12. T. Maitra, M.K. Tiwari, C. Antonini, P. Schoch, S. Jung, P. Eberle, D. Poulikakos, *Nano Lett.* 14, 1 (2014): p. 172-182.
13. H. Zhao, S.J. Park, B.R. Solomon, S. Kim, D. Soto, A.T. Paxson, K.K. Varanasi, A. John Hart, *Adv. Mater.* 31, 14 (2019): p. 1807686.
14. B.R. Solomon, K.S. Khalil, K.K. Varanasi, *Langmuir* 30, 36 (2014): p. 10970-10976.
15. L. Rapoport, B.R. Solomon, K.K. Varanasi, *ACS Appl. Mater. Interfaces* 11, 17 (2019): p. 16123-16129.
16. S.B. Subramanyam, G. Azimi, K.K. Varanasi, *Adv. Mater. Interfaces* 1, 2 (2014): p. 1300068.
17. S.A. McBride, S. Dash, K.K. Varanasi, *Langmuir* 34, 41 (2018): p. 12350-12358.
18. R. Qiu, Q. Zhang, P. Wang, L. Jiang, J. Hou, W. Guo, H. Zhang, *Colloids Surf. A* 453 (2014): p. 132-141.
19. P. Wang, D. Zhang, Z. Lu, S. Sun, *ACS Appl. Mater. Interfaces* 8, 2 (2016): p. 1120-1127.
20. F. Song, C. Wu, H. Chen, Q. Liu, J. Liu, R. Chen, R. Li, J. Wang, *RSC Adv.* 7, 70 (2017): p. 44239-44246.
21. J. Lee, S. Shin, Y. Jiang, C. Jeong, H.A. Stone, C.-H. Choi, *Adv. Funct. Mater.* 27, 15 (2017): p. 06040.
22. T. Xiang, M. Zhang, H.R. Sadig, Z. Li, M. Zhang, C. Dong, L. Yang, W. Chan, C. Li, *Chem. Eng. J.* 345 (2018): p. 147-155.
23. B.R. Solomon, S.B. Subramanyam, T.A. Farnham, K.S. Khalil, S. Anand, K.K. Varanasi, "Lubricant-Impregnated Surfaces," in *Non-Wettable Surfaces: Theory, Preparation and Applications*, eds. R.H.A. Ras, A. Marmur, ch. 10 (London, United Kingdom: RCS, 2016), p. 285-318.
24. B.R. Solomon, X. Chen, L. Rapoport, A. Helal, G.H. McKinley, Y.-M. Chiang, K.K. Varanasi, *ACS Appl. Energy Mater.* 1, 8 (2018): p. 3614-3621.
25. K. Gharbi, F. Salles, P. Mathieu, C. Amiens, V. Colliere, Y. Coppel, K. Phillippot, L. Fontaine, V. Montembault, L.S. Smiri, D. Ciuculescu-Pradines, *New J. Chem.* 41, 20 (2017): p. 11898-11905.